COMMONWEALTH SCIENTIFIC AND INDUSTRIAL RESEARCH ORGANIZATION

DIVISION of FISHERIES and OCEANOGRAPHY

Report No. 67

DESCRIPTION AND PRELIMINARY THEORY OF CIRCULATION IN PORT HACKING ESTUARY

By J. S. Godfrey and J. Parslow

Marine Laboratory
Cronulla, Sydney
1976

COMMONWEALTH SCIENTIFIC AND INDUSTRIAL RESEARCH ORGANIZATION

DIVISION of FISHERIES and OCEANOGRAPHY

Report No. 67

DESCRIPTION AND PRELIMINARY THEORY OF CIRCULATION IN PORT HACKING ESTUARY

By J. S. Godfrey and J. Parslow

Marine Laboratory
Cronulla, Sydney
1976

DESCRIPTION AND PRELIMINARY THEORY OF CIRCULATION IN PORT HACKING ESTUARY

By J. S. Godfrey and J. Parslow

1. INTRODUCTION

Port Hacking estuary lies about 20 km south of Sydney, N.S.W.; the CSIRO Division of Fisheries and Oceanography is at Cronulla Point, near the mouth, so this estuary was chosen in 1973 for an intensive biological and physical study. The work was to be concentrated in South West Arm, since this is surrounded by a National Park and is thus relatively unaffected by human intervention.

Rochford (1951, 1959) studied the climatology of Port Hacking, along with that of many other estuaries, in the 1940's and 1950's; a few of Rochford's results are recapitulated in Section 2. However, Rochford was not specifically concentrating on the dynamics of the estuaries in which he worked, so it was felt appropriate to undertake a new, more intensive study of Port Hacking's circulation. This Report describes observational results so far on the temperature, salinity and current regime, and simple deductions from them. It is hoped that a later report will be devoted to the dissolved oxygen regime.

A bathymetric chart of the area is shown in Fig. 1. The estuary consists of four deep basins — Gunnamatta Bay, Burraneer Bay, South West Arm, and Port Hacking Basin. These are connected with one another and with the ocean via a narrow, shallow tidal channel, whose bed consists of sand brought in from the ocean. Further shallow channels lead to the entrance of the Port Hacking River at Audley, and to two minor streams (Flat Rock Creek entering South West Arm and North West Arm Rivulet). The junctions between the channels and the deep basins are all very well-defined, the depth typically increasing from less than 2 metres in the channels to near the total depth of the basin within a hundred metres.

The Port Hacking River probably accounts for about $\frac{1}{2}$ - $\frac{2}{3}$ of the total freshwater discharge entering the estuary. Since all the other creeks respond to a rainstorm in much the same way as Port Hacking River, we will describe only this stream.

Following a heavy rainstorm, its discharge can rise to a peak value of 100 m^3/sec or more, but this falls within two or three days after the storm down to levels of order 1 m^3/sec; there is a further, slow decrease in dry weather, but the river very rarely dries out completely. However, dry weather flow is of the same order of magnitude as evaporation from the surface of the estuary, so that for perhaps two thirds of the time Port Hacking is essentially an arm of the sea, with undetectable freshwater influence downstream from Lightning Point.

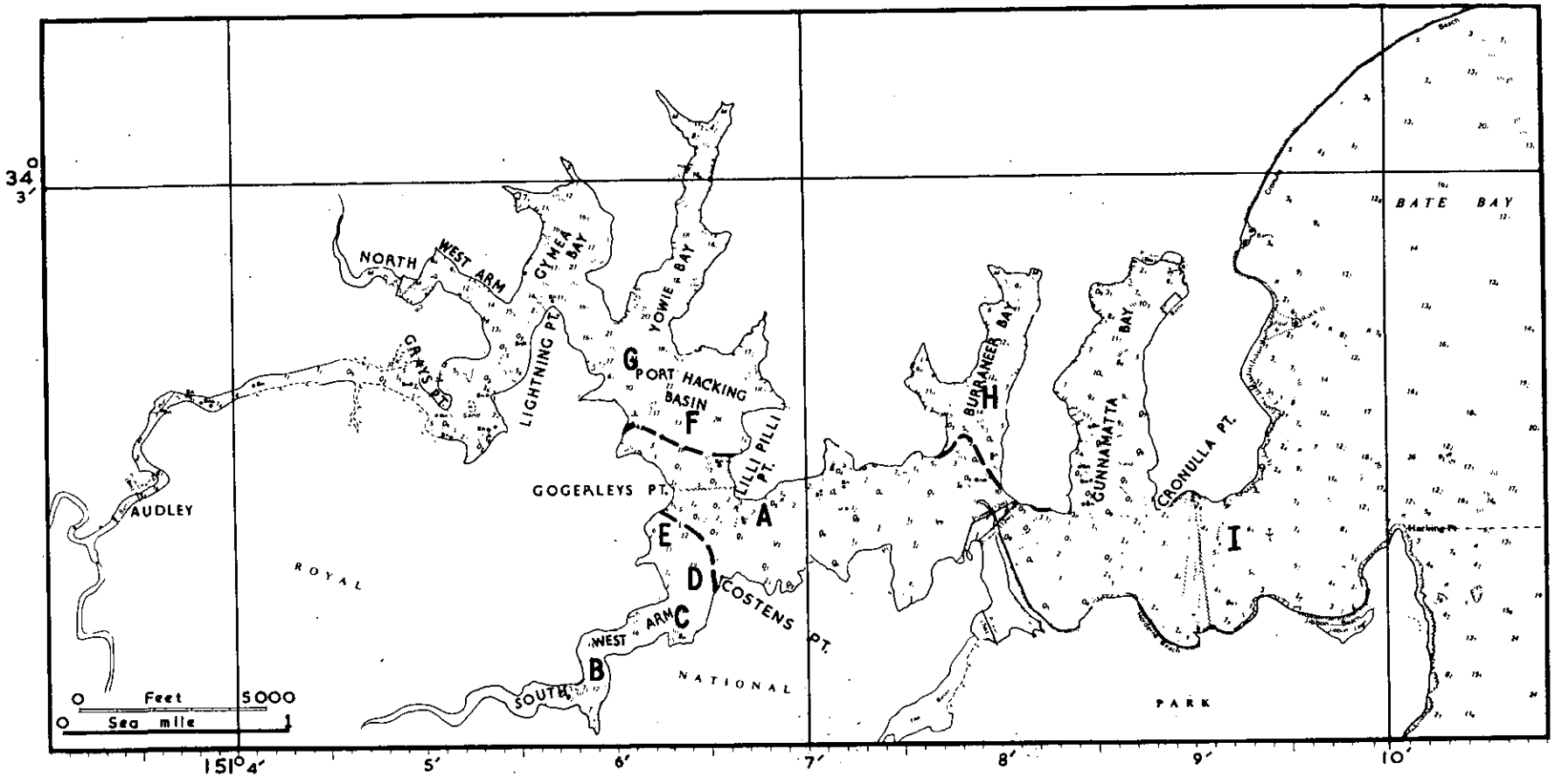

Fig. 1. Port Hacking Estuary. The name "Port Hacking Basin" for the main basin is not an official name. Dashed lines indicate the locations of rising-tide fronts; letters A,B...I indicate the location of hydrographic stations.

At most times — in either wet or dry conditions — the horizontal distribution of temperature and salinity along the estuary is not smooth, but shows large and abrupt changes at a number of fronts. These fronts occur near the junction of the tidal channel with the basins; they are typically less than one metre across, horizontally. The dynamics of the estuary is largely controlled by these fronts. It is thought likely that in any estuary with deep basins connected by shallow channels to the sea (a quite common morphological type around the Australian coast), similar strong fronts are likely to occur. Therefore we have coined the term "front-dominated estuary", to add to the usual list of classification types (e.g., Hansen and Rattray (1966)).

2. SEASONAL TRENDS

The dots in Figs 2a and 2b show the seasonal cycle of temperature at surface and bottom, (16 m), in downstream South West Arm; the data comes from 13 years of monitoring by D. Rochford. A very clearly defined seasonal cycle can be seen in the temperature, both at the surface and bottom. For comparison, the seasonal cycle of temperature at the Port Hacking 50 m station, 5 km out to sea from Cronulla, is also shown (full line, Fig. 2a); estuarine water shows a markedly larger temperature range, particularly at the surface. Furthermore, maximum and minimum temperatures occur about two weeks earlier in the estuary than they do in the ocean.

A similar seasonal scatter diagram of surface salinity (not shown) suggests that for $\frac{3}{4}$ of the time, surface salinity lies in the range 33.0 - 35.5‰, but that deviations down to nearly zero salinity can occur following rainstorms; and in Sydney, these storms can come at any time of year. More will be said on this topic later on. Bottom salinity hardly ever falls below 33‰ — stratification is well-marked, in South West Arm and in Port Hacking Basin.

The rest of this Report is devoted to filling out Rochford's picture of the circulation of Port Hacking. The details of the data collection process are relegated to the Appendix; in this way, the main text can concentrate on the descriptive aspects of the estuary's behaviour.

3. TIDAL BEHAVIOUR

Tides along the central New South Wales coast have a typical range of 2 metres at spring tides, and 1.3 metres at neap tide; there is a moderate degree of diurnal inequality (Fig. 3).

Port Hacking responds to this tidal signal in a rather simple way. For many purposes, one can say that the tide enters all parts of the estuary with no time delays and no loss of amplitude due to friction; to the extent that this is true, mean tidal currents in the tidal

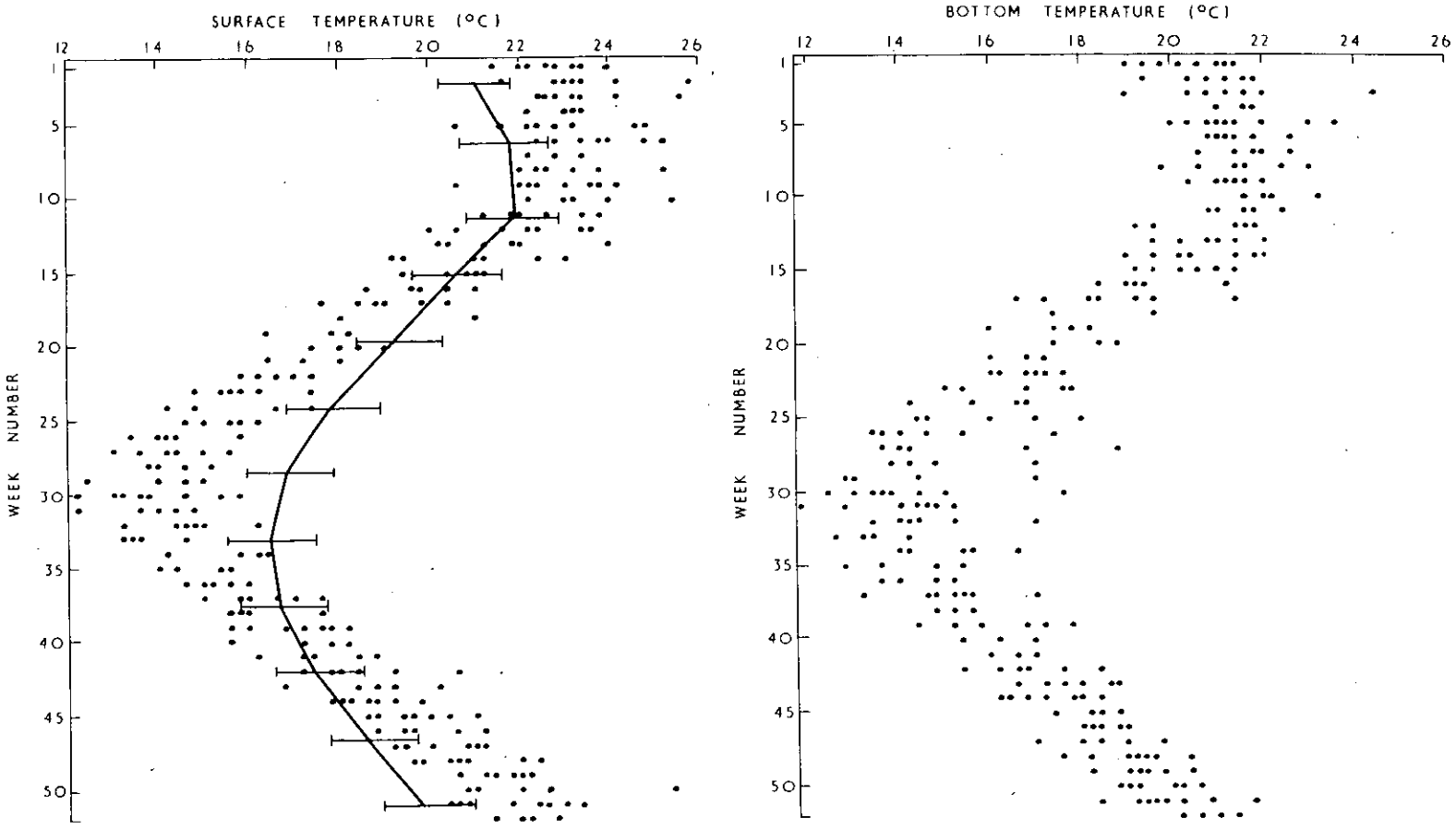

Fig. 2. Observations of water temperature, downstream South West Arm, plotted by week number from 1 to 52, from observations in 1940-1953. (a) Surface temperature. (b) Bottom temperature (about 16 metre depth). For comparison, the full line shows the monthly mean surface temperatures 5 km out to sea from Cronulla 1940-1970; the error bars indicate the standard deviations of these monthly means.

channel south of Lilli Pilli Point can be readily determined by mass continuity. More accurate study shows that high tide in South West Arm is delayed about 10 minutes relative to Cronulla Point, while low tide is delayed about 40 minutes. Even at Audley the tidal amplitude is 0.85 times that at Cronulla, while the tidal delay relative to Cronulla is only about 1 - 1½ hours.

Tidal currents in the entrance channel are strongly turbulent, and they reach 100 cm/sec on a spring tide; however, an abrupt change takes place at the entrance to each of the deep basins, across the fronts. Inside the basins, the tidal flow is quite slow (5 - 10 cm/sec), is laminar, and on a rising tide will quite often take the form of a wedge, entering each basin at a few metres below the surface.

4. RESPONSE TO A RAINSTORM

Many physical processes operating in the estuary reveal themselves rather dramatically after a strong rainstorm; description of rainstorm response therefore forms the core of the report. Rainstorm response has been found to be very reproducible, so what follows is a composite description, built up from observations of several storms. However, it is illustrated mainly from one very large rainstorm on 10th - 13th March 1975 during which 174 mm of rain fell at Cronulla (Fig. 5a).

4.1 *Initial response*

The normal condition of the river channel from Audley to Grays Point is like a miniature fjord, with estuarine circulation confined to the top 2 metres; water below this depth is purely marine (salinity near 35‰), and is almost motionless. However, when a sufficiently strong rainstorm develops, the river channels become completely flushed of salt water within a few hours; Agnew and Imberger (1974) found very similar behaviour in the Blackwood River, Western Australia, between the summer dry season and the winter wet.

It is easy to deduce a limiting value of discharge, above which the channel must be completely flushed. Above 70 m^3/sec, the top layer of a two-layer flow at Grays Point would have to move downstream at a speed (u) greater than 70 cm/sec, to carry the fresh water seawards. Even if the fractional density difference $\Delta\rho/\rho$ were as large as 0.02, such a flow would be dynamically unstable — the internal Froude number, $u^2/g\frac{\Delta\rho}{\rho}H$, would be greater than unity (H is upper layer depth, ~ 1 metre). In fact, the river discharge above which complete flushing takes place is probably considerably less than 70 m^3/sec.

Within the first few hours following rain, the freshwater discharge spreads as a thin sheet over the two inner basins; the Port Hacking and North West Arm Rivulet outflows spread over Port Hacking Basin, and the Flat Rock Creek discharge spreads over South West Arm. Below each freshwater sheet (which may be only 50 cm thick, after a minor storm)

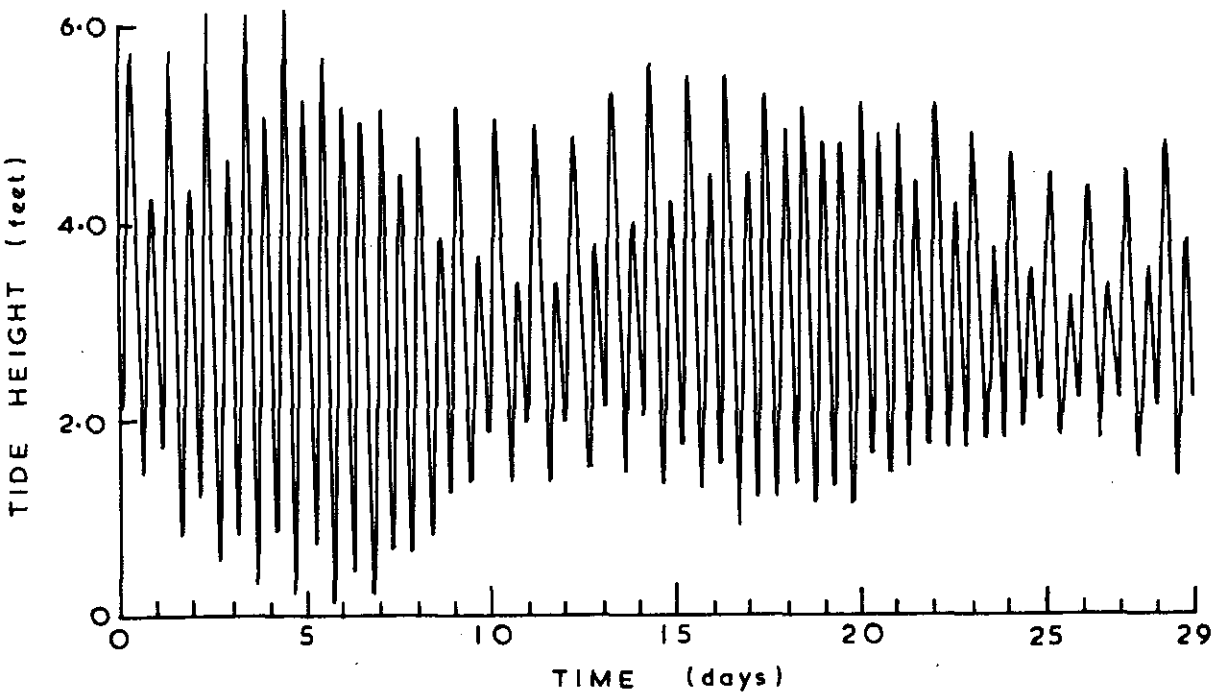

Fig. 3. Recorded tides, Camp Cove, Sydney Harbour, September 1967. From "The Tides of the Continent of Australia", A.K. Easton (1970).

the salinity profile is initially unaffected. Horizontal tows of a salinity sensor during such storms show the surface salinity in each basin to be patchy, with regions of constant salinity a few hundred metres wide, separated from one another by sharp "fronts". Frontal movements are often made visible by differences in silt concentration; speeds are generally of order 10 cm/sec. Such frontal speeds are consistent with the movement of the nose of an internal gravity current over still water (Turner, 1973, Section 3, 2, 5); by this gravity current mechanism, a freshwater layer can spread over an entire basin within two or three hours.

4.2 *The rising-tide fronts*

As already noted, flow in the tidal channel is turbulent and can reach 100 cm/sec. This has two consequences of importance. First, at such speeds water entering the two inner basins at the peak of high tide should have originated well out in Bate Bay, a few hours earlier; it therefore has near oceanic salinity. Second, internal gravity currents are not nearly fast enough to propagate down the channel during a rising tide. Consequently, after a rainstorm, dense, salty water enters the basins, and an intense front develops between it and the fresher water inside. The tidal inflow immediately falls several metres down the steep inner sandbanks in a turbulent plume; it entrains a certain volume of water from inside each basin, and the mixture then spreads into the basin at some intermediate depth. This behaviour is particularly well-marked in Port Hacking Basin, where the front runs accurately parallel to the lip of the sandbank right across the entrance of the basin, about 100 metres upstream (dashed line, Fig. 1). One diving expedition has established that the saltwater does, indeed, fall straight down the sandbank — an angle to the horizontal of order 30°.

The whole phenomenon is strongly reminiscent of the laboratory experiments of Ellison and Turner (1959) (see also Turner, 1973). The entrainment ratio E (i.e., the ratio of flow speed towards the front within the fresh layer to flow speeds within the plume itself) is thought to be of order 0.1 - 0.2, though more detailed observations are needed to check this. Following heavy rain, the fronts will be marked by a line of debris so thick that an outboard motor is invariably clogged in trying to pass through; the water surface rises and falls a few centimetres, as if at a rolling boil.

4.3 *The falling-tide fronts*

When the point of high tide is reached, the rising-tide fronts move bodily downstream with the tide and are broken up by turbulence; within one or two hours, new fronts appear. These are not quite so constant in pattern as the rising-tide fronts, but one type in particular is noteworthy, as it illustrates the complexity of the tidal mixing process. This front starts at location * and extends downstream and across to Lilli Pilli Point (Fig. 4). What happens is that the sandbanks surrounding the trough at * allow only the fresh

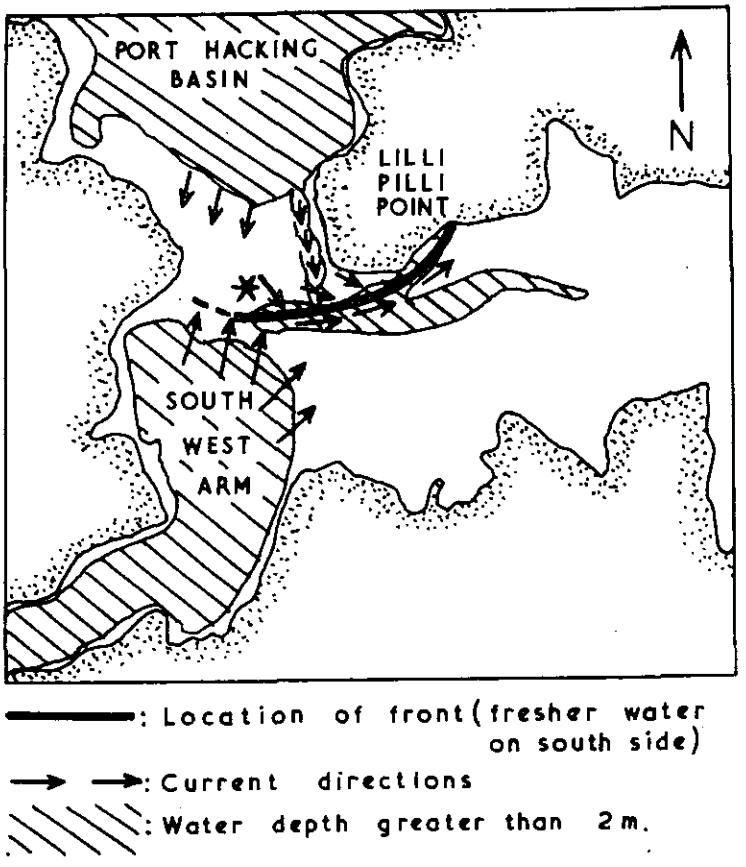

Fig. 4. Falling-tide front off Lilli Pilli Point. Fresh water accumulates in the deep hole at *, then rises up and over the salty water coming through the channel just west of Lilli Pilli Point.

surface water, from the top of Port Hacking Basin and South West Arm, to flow seaward on a falling tide. On the other hand, relatively deep, salty water from Port Hacking Basin flows rapidly through the channel beside Lilli Pilli Point, and is vertically mixed by turbulence; the front forms where the two water bodies meet one another. The fresher water rises up and over the saltier water as both move downstream, so the front reaches the shore at Lilli Pilli Point. A mat of debris some hundreds of square metres in extent will form at the junction, following rain. Further downstream, tidal turbulence mixes the water vertically, so that by the time the water passes Burraneer Point (typically an hour after leaving the basins) it is usually homogeneous both vertically and horizontally.

It is worth noting that these fronts make the choice of monitoring stations quite difficult. One has to be careful in interpreting data from a station anywhere near a front. Even in dry summer weather, the fronts are often present, in their usual locations, and show up sharply on a temperature recorder; but they are not visible. It is only by learning where the fronts are likely to be and avoiding such places that one can get readily interpretable data.

4.4 *Deepening and mixing within the basins*

During the first few days after a storm, the fresh water "pulse" that entered during the storm passes down the tidal channel several times, and becomes mixed with ocean water. Much of the mixed water returns to the basins in the first few hours of each rising tide, and sinks with the rising tide fronts; the net effect is to mix the fresh water layer — initially present in the basins only in the top metre or so — down to 4 metres or deeper. This can be seen by careful inspection of Fig. 5b — salinity at 4 metres is still close to 35‰ on 10th March, but has fallen to a minimum by 12th March. After that time, Fig. 5b suggests that the salinity rises almost exponentially back to marine values, both at 0 metres and at 4 metres. The breakdown of the "exponential" rise around 1st April is thought to be due to cold westerly winds on that day, which caused the strong cooling and mixing evident in Fig. 5c.

The deepening of the salinity profile is illustrated more fully in Fig. 6, which shows various profiles of the "salinity deficit" (i.e., 35‰ minus observed salinity) at the downstream South West Arm station, normalized to unity at 1 metre depth. On the first day of heavy rain, 10th March, the normalized salinity deficit at the surface is 8.0 (profile not shown); but by 12th March, a much smoother profile has developed. Progressive deepening of the profile can be seen, as time increases, but it is slow enough that a single average profile function $f(z)$ — dotted line, Fig. 6 — describes the salinity profile reasonably well throughout the period 12th March - 24th March.

It is implied above that in the absence of strong winds, the deepening process is due to mixing of fresh and salt water in the tidal channel, with subsequent redistribution in depth at the rising-tide

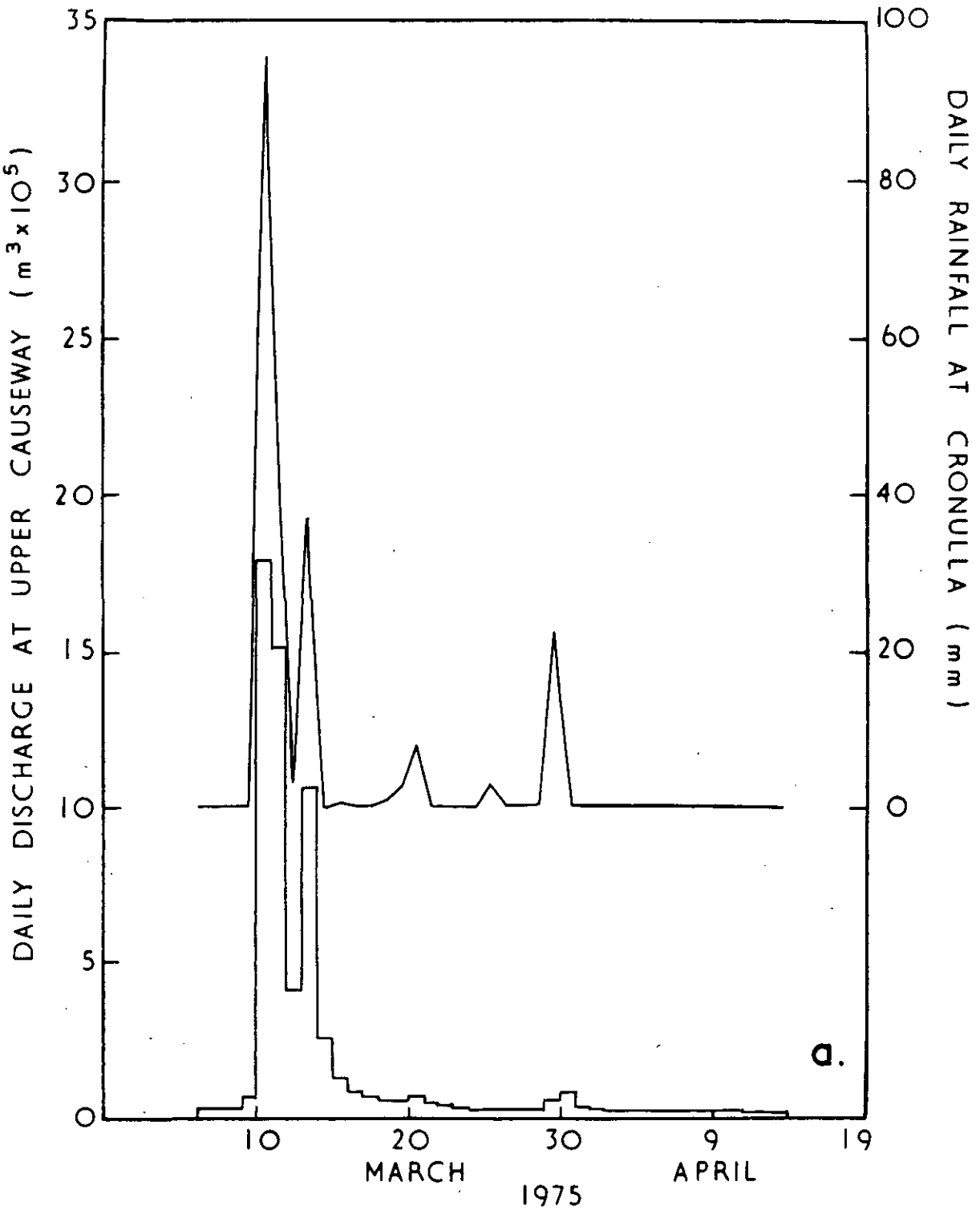

Fig. 5a. Daily rainfall at Cronulla, and Port Hacking River discharge at Upper Causeway, 7 km upstream from Audley. Total discharge into Port Hacking Basin is probably about twice the value at Upper Causeway.

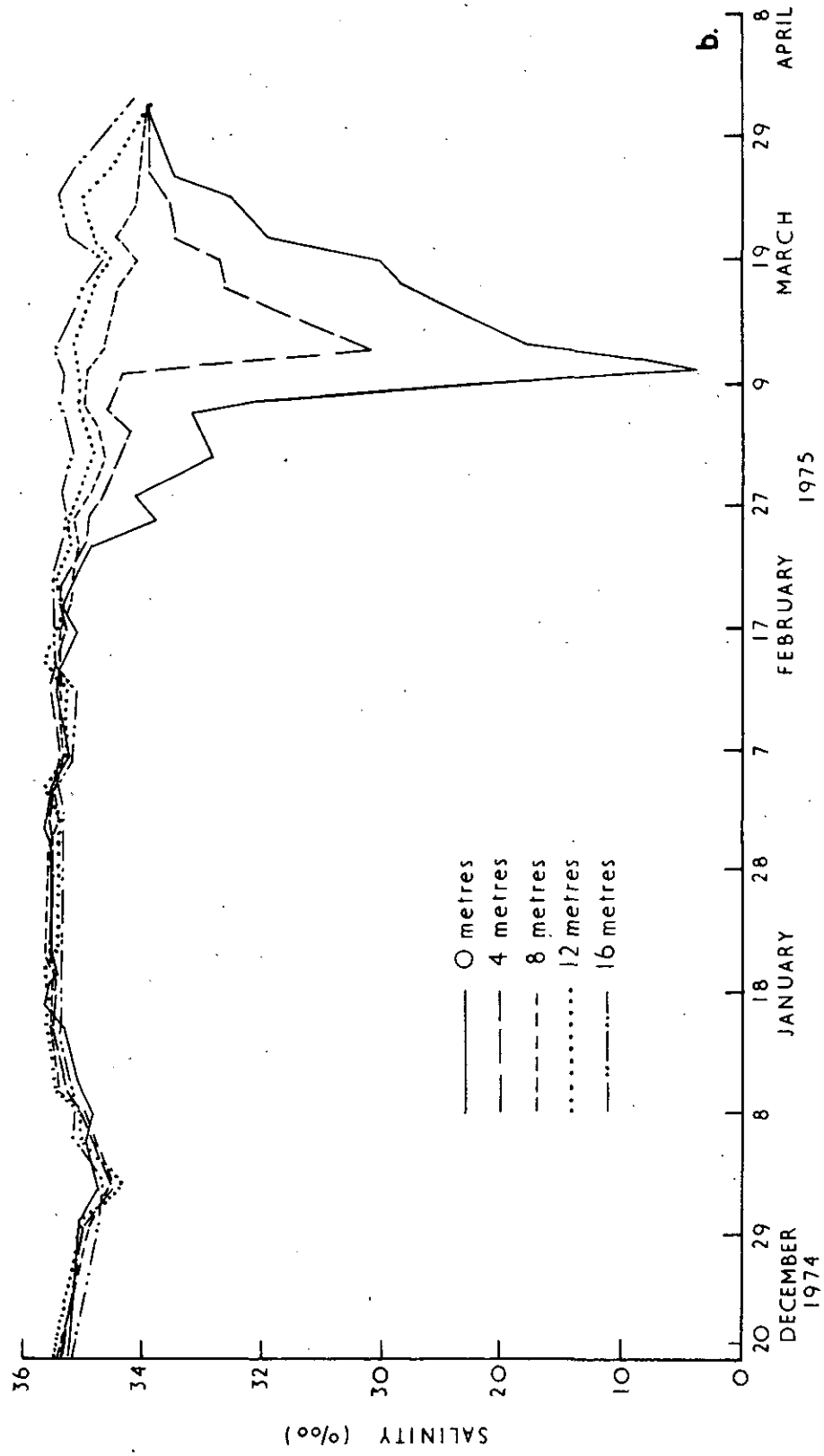

Fig. 5b. Salinity at various depths, downstream South West Arm. Note the change in the salinity scale at 30‰.

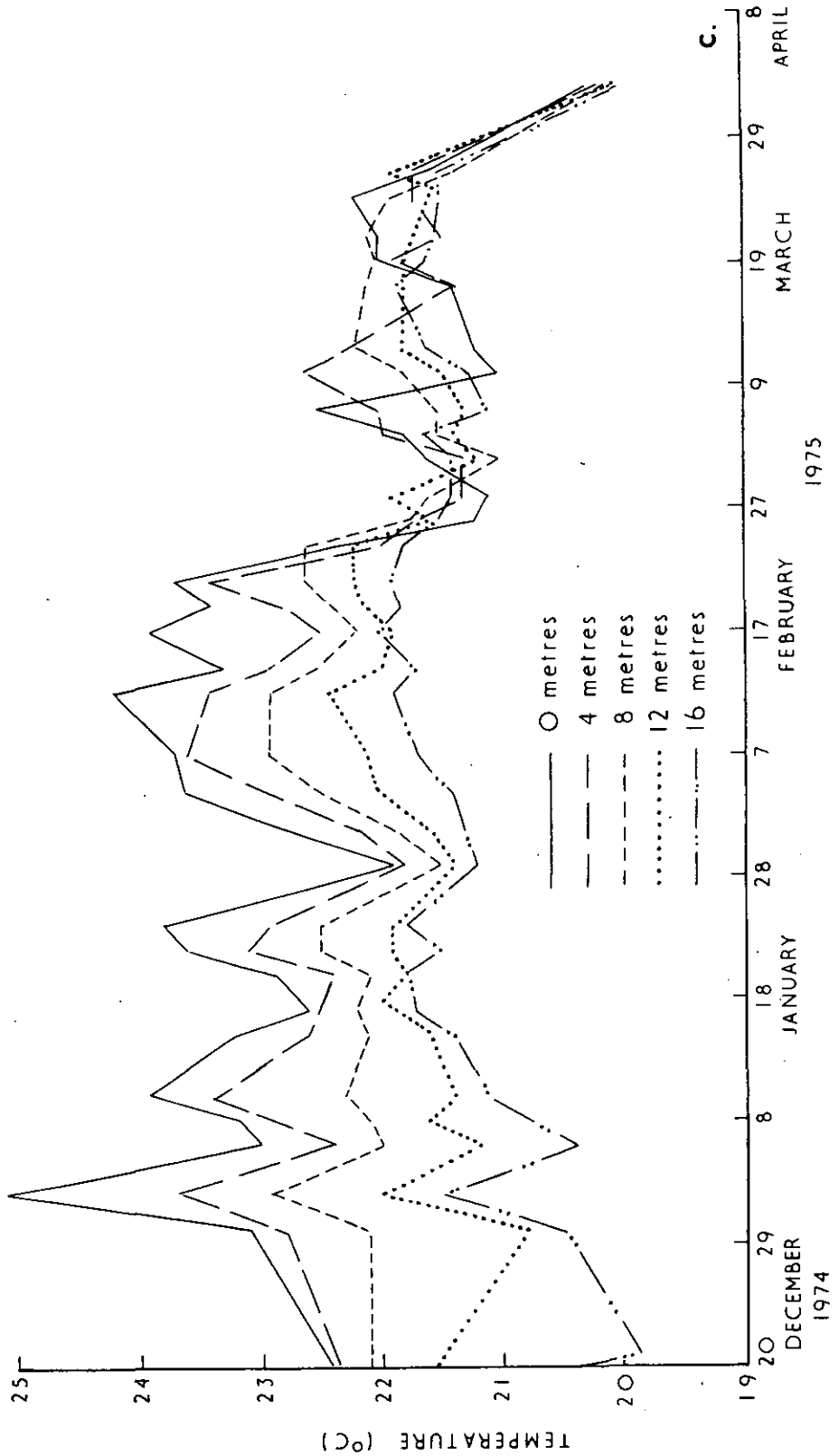

Fig. 5c. Temperatures at various depths, downstream South West Arm.

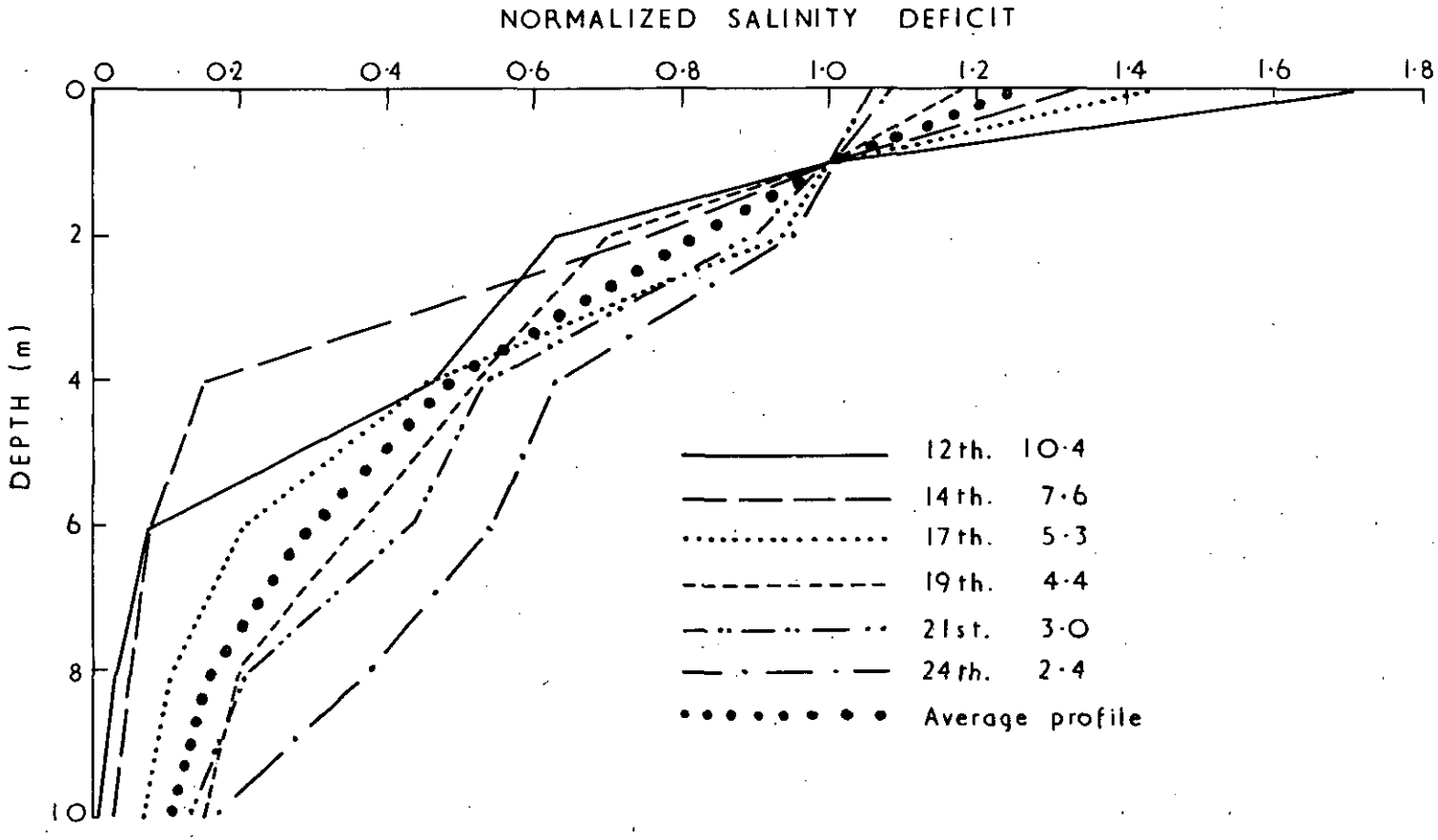

Fig. 6. Profiles of salinity deficit (i.e., 35‰–observed salinity), at downstream South West Arm, normalized to unity at 1 m; actual magnitudes of salinity deficits at 1 m are shown in the figure, e.g. the deficit on 12th March was 10.4‰. Note the steady deepening of the profiles after the rainstorm of 10th-13th March. The dotted line is the "average" profile adopted in the theory of Section 4.6.

front. While this is certainly an important mixing mechanism, we cannot prove it is the *only* one. However it seems unlikely that turbulent mixing within the basin is important. The low level of turbulence inside the basins can be illustrated by hanging a 5 cm x 5 cm piece of porous cardboard, impregnated with fluorescein, from a small float at a depth of (say) 2 metres in either basin. A track is laid out as the float drifts over the surface, leaving a thin, laminar line of fluorescein visible for 15 minutes after the float is inserted. Strong vertical mixing seems unlikely in such an environment.

4.5 *Density currents and horizontal homogeneity within the basins*

The tracking of miniature drogued buoys, with fluorescein-impregnated cardboard at the drogue to improve visibility, is a useful technique in such clear, calm waters. Such studies reveal undercurrents of up to 15 cm/sec going upstream, at depths of 2 - 4 metres or more, during the rising tide; during this time, surface water is generally moving slowly *downstream* at speeds of order 5 cm/sec. Since the velocity of water entering the basins over the shallows is typically 25 - 50 cm/sec when it reaches the front, the entrainment ratio E = (velocity of drift towards the turbulent plume)/(velocities within the plume) is probably of order 0.1 - 0.2, somewhat higher than the values found by Ellison and Turner (1959) for plumes flowing down slopes of about 30°.

With density currents of order 5 - 10 cm/sec acting directly to produce horizontal homogeneity, it would be expected that the density field itself would be highly homogeneous in the horizontal, within each basin. This is generally true, as can be seen in Fig. 7: this shows the density anomaly at two stations in South West Arm, plotted at various near-surface depths. Before the storm of 10th March, horizontal homogeneity holds to within the accuracy of the S/T meter, below 1 metre depth. After the storm, the density patterns at each station are very similar; the intuitively-expected tendency for upstream water to be lighter (less salty) than downstream water at a given depth can be seen, but it is remarkably slight. There are many occasions on which the upstream water is in fact *denser* than downstream. Below 8 metres the density field is completely homogeneous in the horizontal, to the accuracy of the meter†. Similar conclusions hold in Port Hacking Basin, although here the greater freshwater inflow results in frequent reductions of salinity of order 2‰ at an upstream station in Port Hacking Basin, relative to a down stream station, in the top 2 metres.

†Quite often, however, the salinity and temperature fields individually will *not* be perfectly horizontally homogeneous; water at one end will be noticably colder and fresher than at the other. Such inhomogeneities do not induce self-correcting density currents.

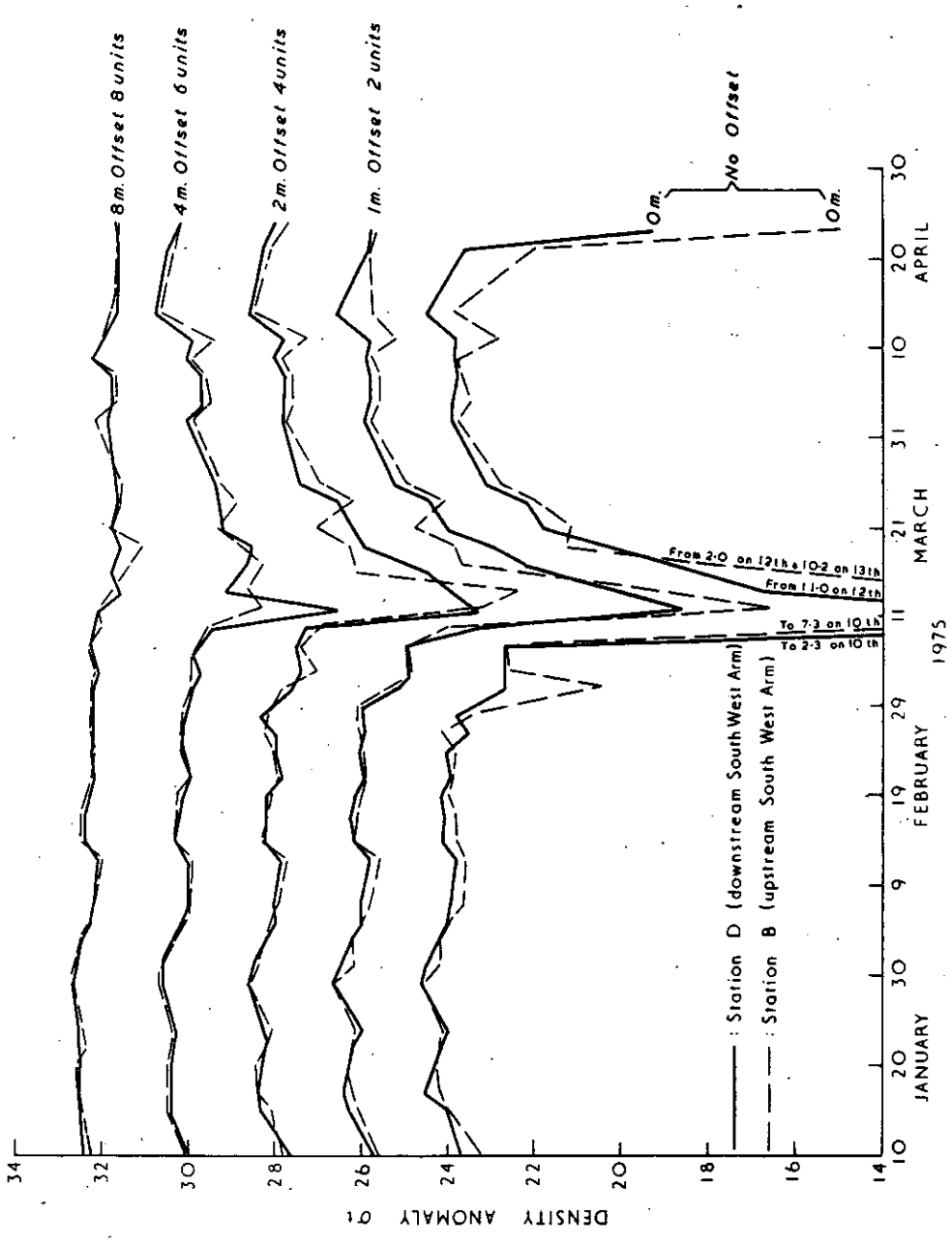

Fig. 7. Density anomaly σ_t, at two stations in South West Arm, at various depths. Each pair of graphs is offset two units compared to the one below it. Note the high degree of horizontal homogeneity.

4.6 *A simple theory of tidal flushing*

We have seen that the salinity distribution after a rainstorm is roughly homogeneous horizontally within each basin, and it can be described by the profile function f(z) (dotted line, Fig. 6). This allows us to simplify the description of each basin considerably. If $S_i(x,y,z,t)$ is the salinity at horizontal position (x,y) in the i th basin at depth z and time t, then we can define variables q_1 and q_2 by

$$(35‰ - S_i(x,y,z,t))/35‰ = q_i(t)f(z) \qquad (1)$$

where i = 1,2 refer to Port Hacking Basin, South West Arm respectively. Thus the salinity structure of the entire 2-basin system can be described approximately in terms of two variables — $q_1(t)$ and $q_2(t)$. Two simultaneous equations involving these quantities will now be derived by considering the flushing of freshwater from the 2-basin system. The freshwater content of basin i is

$$F_i(t) = \int \frac{(35‰ - S(x,y,z,t))dx\ dy\ dz}{35‰}$$

$$= q_i(t)\int A_i(z)f(z)dz$$

$$\simeq \bar{A}_i\ q_i(t)\int_0^\infty f(z)dz$$

where A_i is the area of basin i at depth z, and $\bar{A}_i$ is the surface area of basin i, or

$$F_i(t) = V_i q_i(t)$$

where

$$V_i = \bar{A}_i\int_0^\infty f(z)dz \qquad (2)$$

Let q_{in} be the value of $q_i(t)$ at the n th high tide. Then $V_i(q_{in+1}-q_{in})$ is the total amount of freshwater flowing into the i th basin between the n th high tide and the (n+1)th. This is made up of two contributions; the first is the direct freshwater inflow into the i th basin, R_{in}, which is assumed to be known from river gauging and rainfall measurement. The other is the loss of freshwater by flushing out to sea.

If the tidal range (assumed constant, for simplicity) is h metres and the depth of sill is H metres at high tide, then on the falling tide the top H metres of each basin should be thinned down to (H-h), resulting in a loss of freshwater (for the i th basin on the n th falling tide) of

$$\bar{A}_i\ h\ q_{in}\int_0^H f(z)dz/H = V_i'\ q_{in}. \qquad (3)$$

(Order of magnitude estimates suggest that "drawdown" effects, in which water from below the sill is pulled up and over the sill during falling tide, are not important unless water in the basins is already close to marine salinity – see for example the section on selective withdrawal in Turner, 1973).

During the falling tide, water from both basins enters the tidal channel and mixes, so that at the start of the rising tide, water returning to *either* basin has salinity

$$S_{mix} = (S_{1n}V_1' + S_{2n}V_2')/(V_1' + V_2'). \qquad (4)$$

As the tide rises and water from progressively further out to sea makes its way into the two basins, the salinity of the entering water also rises. Clearly, the flushing characteristics of the estuary depend sensitively on how rapid this rise of salinity is: if the salinity in the channel remained at S_{mix} throughout the rising tide, the two basins would merely equalize in salinity and would never flush out to sea; on the other hand if the salinity returned to marine values in the channel as soon as the tide began to rise, all the fresh water would flush out of the estuary in one or two tidal cycles.

Unfortunately, information on this aspect of the estuary's behaviour can only be found empirically. The limited observations available suggest that the salinity of inflowing water remains at about S_{mix} while the tide rises $l_1 = 0.3$ metres; it rises linearly to ocean salinity (35‰) when the tide rises a further $l_2 = 1$ metre; and remains constant at ocean salinity after that. Hence the freshwater content entering the i th basin (assuming the tide rises a total of 1.3 metres or more) is approximately

$$\bar{A}_i \, q_{mix}(l_1 + \tfrac{1}{2} l_2) = V_i'' \, q_{mix} \qquad (5)$$

where $q_{mix} = (35‰ - S_{mix})/35‰$.

Adding together all the contributions, we find for the change in freshwater content of the i th basin between the n th an (n + 1)th high tides

$$V_i(q_{in+1} - q_{in}) = R_{in} - V_i' q_{in} + V_i''(q_{1n}V_1' + q_{2n}V_2')/(V_1' + V_2'), \text{ for } i = 1,2. \qquad (6)$$

This provides two linear equations with constant coefficients for the two unknowns q_{1n}, q_{2n}; they are therefore readily soluble.

It is convenient to divide (6) by V_i, noting that

$$V_1'/V_1 = V_2'/V_2 = \delta = h/\int_0^\infty f(z)dz; \quad V_1''/V_1 = V_2''/V_2 = \delta' = (l_1 + \tfrac{1}{2}l_2)/\int_0^\infty f(z)dz.$$

The equations become

$$q_{1n+1}-q_{1n} = R'_{1n}-\delta q_{1n}+\delta'\bar{q}_n \tag{7}$$

$$q_{2n+1}-q_{2n} = R'_{2n}-\delta q_{2n}+\delta'\bar{q}_n \tag{8}$$

where $\bar{q} = (V'_1q'_1+V'_2q'_2)/(V'_1+V'_2)$; $R'_i = R_i/V_i$.

4.7 *Solutions and comparison with observation*

Define $\Delta = q_1-q_2$; then subtracting (8) from (7) gives

$$\Delta_{n+1} = (dR')_n+(1-\delta)\Delta_n \tag{9}$$

with the solution $\Delta_n = \sum_{j=1}^{n-1}(dR')_j(1-\delta)^{n-1-j}+\Delta_0(1-\delta)^n$ (10)

where $(dR')_j = R'_{1j}-R'_{2j}$, and Δ_0 is the value of Δ at the initial high tide.

Next, multiply (7) by $V'_1/(V'_1+V'_2) = \bar{A}_1/(\bar{A}_1+\bar{A}_2)$,

(8) by $V'_2/(V'_1+V'_2) = \bar{A}_2/(\bar{A}_1+\bar{A}_2)$,

and add; we obtain an equation for the area-averaged salinity deficit, $\bar{q}$, namely

$$\bar{q}_{n+1} = \bar{R}'_n+(1-\delta+\delta')\bar{q}_n, \tag{11}$$

with the solution $\bar{q}_n = \sum_{j=1}^{n-1}\bar{R}'_j(1-\delta+\delta')^{n-1-j}+\bar{q}_0(1-\delta-\delta')^j$ (12)

where $\bar{R}'_j \simeq (\bar{A}_1R'_{1j}+\bar{A}_2R'_{2j})/(\bar{A}_1+\bar{A}_2)$ and $\bar{q}_0$ is the value of $\bar{q}$ at the initial high tide. $\bar{R}'_n$ is the total freshwater to enter the estuary per unit area, between the n th and (n+1)th high tides.

The nature of the solution is illustrated by considering a hypothetical special case, in which river flow somehow generates a situation with South West Arm purely marine, and with a salinity deficit in Port Hacking Basin distributed according to the profile function f(z) and with $q_{10} = 1$. We suppose further that river inflow into both basins is zero after the initial instant. The solution in this case is

$$q_{1n} = \left[\bar{A}_1(1-\delta+\delta')^n+\bar{A}_2(1-\delta)^n\right]/(\bar{A}_1+\bar{A}_2) \tag{13}$$

$$q_{2n} = \bar{A}_1\left[(1-\delta+\delta')^n-(1-\delta)^n\right]/(\bar{A}_1+\bar{A}_2) \qquad (14)$$

which are displayed in Fig. 8 for numerical values of the constants deduced from the data given earlier namely

$$\delta = h/\int_0^\infty f(z)dz \simeq \frac{1}{4}\ , \qquad (15)$$

$$(\delta-\delta') = (h-l_1-\tfrac{1}{2}l_2)/\int_0^\infty f(z)dz \simeq \frac{1}{12} \qquad (16)$$

and $$\bar{A}_1 = 3 \times 10^6 m^2, \quad \bar{A}_2 = 10^6 m^3.$$

Note that the difference in salinity between the two basins decays rapidly, with an e-folding time of about 4 tidal cycles; whereas the area-average salinity returns exponentially and relatively slowly to marine values, with an e-folding time of about 12 tidal cycles. This seems a fair representation of real behaviour; after a sharp storm the salinity in the two basins does remain rather close together, with Port Hacking Basin usually somewhat fresher. Furthermore, a logarithmic plot of area averaged salinity deficit at 1 metre depth versus time, for the period following the 10th March storm is shown in Fig. 9; the plot is surprisingly close to linearity, with an enfolding time of 7.5 days, or 14 tidal cycles. Data from 2 other smaller storms yield somewhat less accurate straight lines, but nevertheless exponential-type decay was found in each case with e-folding times of 7 - 10 days.

5. TEMPERATURE STRUCTURE DURING DRY PERIODS

There are periods of several months at a time in which little rain falls over the Port Hacking catchment, and salinity remains close to 35‰ throughout the inner two basins. The temperature structure in South West Arm in one such period (20th December 1974 - 5th March 1975) is shown in Fig. 5c and Fig. 10. Marked thermal stratification is evident, with large fluctuations in time. In this section, we consider what causes these fluctuations.

A number of studies have been published recently, concerning time changes in the temperature structure of lakes and of quiet, horizontally homogeneous parts of the ocean (e.g., Kraus and Turner (1967), Denman and Miyake (1973), Edwards and Darbyshire (1973)). It appears that the basic elements of the process are now understood. Direct heating by the visible-band component of solar irradiation needs special attention: the depth distribution of this heating must be determined by direct observation, since it depends on water turbidity. All other heating and cooling effects may be treated as surface phenomena; this includes the infrared component of solar heating, thermal radiation into and out of the water column, evaporative and sensible heat losses. The mixing of these heat inputs over depth is

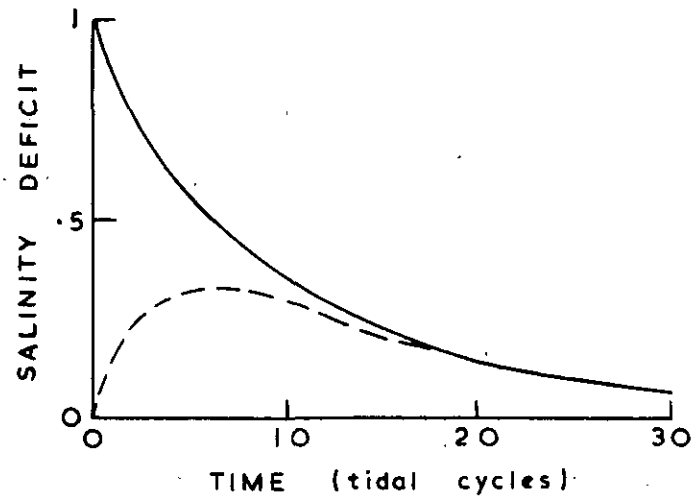

Fig. 8. Solution of the salt budget equations (7) and (8) for the salinity deficit, in a hypothetical case for which Port Hacking Basin initially has a deficit of unity and South West Arm is purely marine. Full line: Port Hacking basin; dashed line: South West Arm.

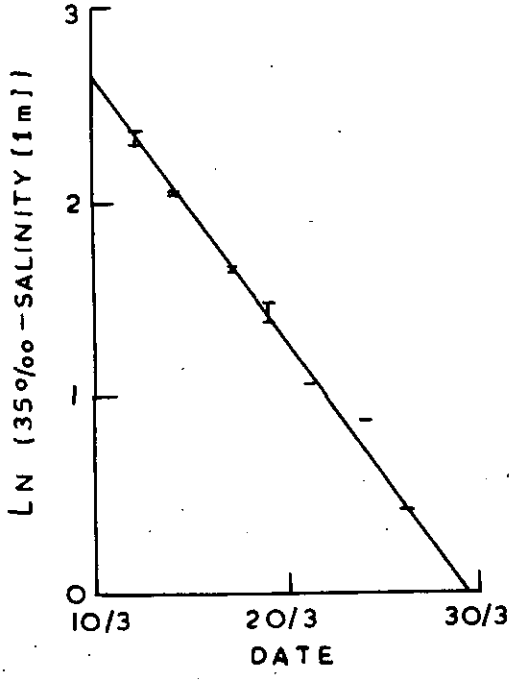

Fig. 9. Logarithmic plot of salinity deficit at 1 m depth, South West Arm, following the March 10th storm. The slope of the graph corresponds to an e-folding decay time of 7.5 days, or 14.4 tidal cycles.

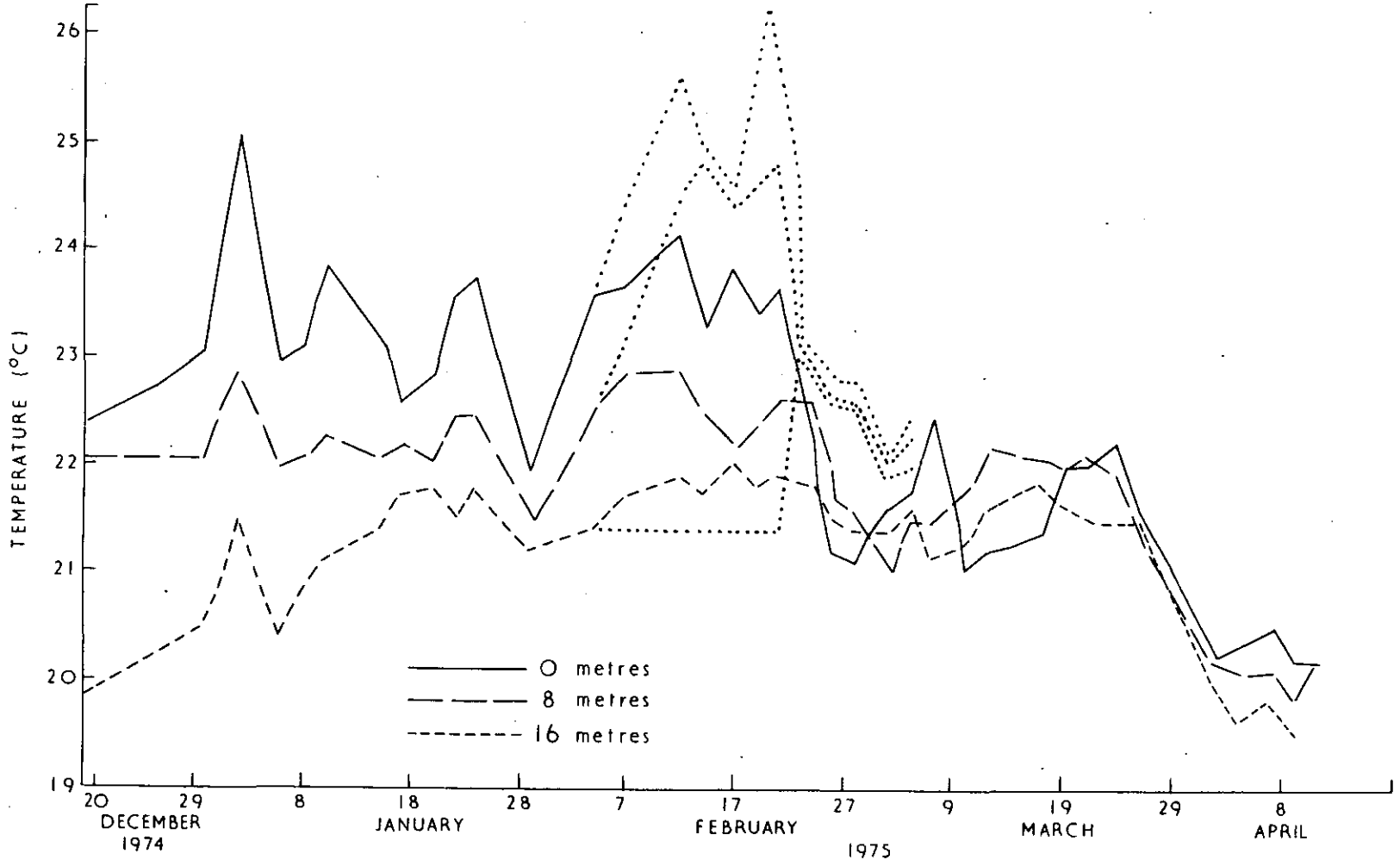

Fig. 10. The full and dashed lines are observed temperatures at 0, 8 and 16 m, from downstream South West Arm, (repeated from Fig. 5c). The dotted lines are predicted temperatures, based on a multilayer model which treated South West Arm essentially as a lake, and ignored tidal exchange of heat.

mainly performed by wind-induced turbulence, which periodically creates a "homogeneous mixed layer". Below this layer, mixing is relatively slight. The rate of wind mixing is given to rough approximation by the rule that a constant fraction (of order $10^{-2} - 10^{-3}$) of the work done by the wind on the water is used to create the mixed layer, thereby raising the potential energy of the water column. Since the work done increases as the cube of the wind speed, mixed layer formation occurs mainly during gales.

There is, however, another mixing mechanism commonly included in studies of water temperature structure: when the water column is made dynamically unstable by surface cooling, convection will take place. This will also tend to deepen the surface mixed layer.

A numerical model based on these ideas, in which South West Arm was treated essentially as an isolated lake, was run between 4th February and 5th March 1975; the necessary data on wind speed, air temperature and humidity, and solar radiation were taken from a weather station at Cronulla. Details of the model will be given in a later paper. The model results are shown as dotted lines in Fig. 10. It is apparent that the model predicts greater heating in South West Arm than actually occurred, but the pattern of stratification as a function of time is quite well reproduced; in particular, the sudden fall of temperature and stratification on 23rd February is due to cold, dry westerly winds around that time, causing large sensible and latent heat losses, convective mixing, and some wind mixing.

However, it is not worth trying to adjust the parameters of this simple model to fit the observations better, if the model omits a major term in the heat balance: and the tidal exchange of heat is probably a major term. To see this, note that in summer, marine water is typically $1^{o} - 2^{o}C$ colder than estuarine water (see Fig. 2a), and some of this water reaches the inner two basins on each rising tide. The seasonal regularity of this tidal exchange process shows up well in the output of a temperature recorder off Cronulla Point (courtesy D.Smith). In summer and winter, a rather regular tidal cycle appears in the temperature trace; in summer, lowest temperatures occur near high tide, while in winter, they occur near low tide. The amplitudes are roughly what one would expect from inspection of Fig. 2a, if South West Arm water lay off Cronulla Point at low tide and ocean water lay off the point at high tide.

In summer, on the rising tide, the colder, denser water sinks at fronts at the entrances of the two basins; the fronts are just as sharp as those described in Section 3.2, and occur in essentially the same locations. It therefore seems reasonable to estimate the cooling rate due to tidal exchange by assuming that an equation similar to (11) holds for the area-averaged temperature structure in dry conditions, i.e., we assume that if $\overline{\tau}_n$ is the near surface temperature averaged over both basins, at the n th high tide, then

$$\overline{\tau}_{n+1} - \overline{\tau}_n \simeq (\text{source terms}) - (\delta - \delta')(\overline{\tau}_n - \sigma_n). \qquad (17)$$

The "source terms" are the direct heating effects that have already been included in the calculated curves, Fig. 10; the second term on the right of (17) represents tidal exchange. It is proportional to the difference between the temperature $\overline{\tau}_n$ inside the estuary and the ocean temperature σ_n; the estimate $(\delta-\delta') \simeq \frac{1}{12}$ (tidal cycle)$^{-1}$ of the proportionality constant is probably too large, because temperature is not distributed with depth according to the average profile f(z) of Fig. 6. Nevertheless, (17) will serve to estimate order of magnitudes. With $(\overline{\tau}_n-\sigma_n) \sim 2^oC$, and $(\delta-\delta') \sim$ (6 days)$^{-1}$, we find a cooling rate of $\frac{1}{3}\,^oC$/day – comparable to observed rated of change of temperature in Fig. 5c. Thus the tidal exchange of water must be accounted for in any quantitative model of water temperature and salinity in Port Hacking; a model of this kind is under development, and will be reported in a later paper.

6. SUMMARY

Port Hacking Estuary consists of a number of basins, connected to the sea by a shallow tidal channel, in which vigorous vertical and lateral mixing takes place. After a rainstorm, approximate horizontal homogeneity is quickly achieved in each basin. On a falling tide, fresh surface water is skimmed from the top of each basin, and is partially mixed with marine water in Bate Bay. On the returning tide, the mixed water sinks below the fresher surface water inside each basin, and spreads inwards via internal gravity currents, at typical depths of 2 - 6 metres. Entrainment of freshwater takes place across the rising tide plume. The salinity profile deepens slowly as a result of this process; however, a single time-average profile fits the observations quite well for much of the time. This allows development of a very simple theory of freshwater flushing from Port Hacking Estuary, which predicts exponential decay of freshwater content at roughly the observed rate.

The same general physics holds for exchange of heat between the estuary and the ocean, particularly in summer; however, the details of the turbulent mixing occurring in the rising-tide fronts now need to be taken into account, because dry-weather temperature profiles are not shaped like wet-weather salinity profiles. In other words, a theory is needed which predicts the vertical profiles, instead of assuming they have a constant shape as in the theory of Section 3. Such a theory is under development at present.

Acknowledgements

This study would not have been possible without help from large numbers of people. Mr P. Hibel did most of the hydrological observations; Messrs H. Jitts and B. Scott provided the radiation data; Mr M. Greig performed the tidal analysis; and Messrs B. Griffiths and W. Fitzgerald assisted in diving. In addition, valuable advice was received from Professor J.S. Turner and from Mr P. Stone.

7. REFERENCES

Agnew, H., and J. Imberger (1974). Tidal dynamics in a typical estuary of the south-west coast of Western Australia. Fifth Australasian Conf. on Hydraulics and Fluid Dynamics.

Denman, K.L., and M. Miyake (1973). Upper-layer modification at ocean station Papa, observations and simulation. *J. Phys. Oceanogr.* 3, 185-196.

Easton, A.K. (1970). "The Tides of the Continent of Australia". (Horace Lamb: Adelaide).

Edwards, A., and J. Darbyshire (1973). Models of a Lacustrine Thermocline. Fourth Liège Colloquium on Ocean Hydrodynamics, pp. 81-102.

Ellison, T.H., and J.S. Turner (1959). Turbulent entrainment in stratified flows. *J. Fluid Mech.* 6, 423-428.

Hansen, D.V., and M. Rattray, Jr. (1966). New dimensions in estuary classification. *Limnol. Oceanogr.* 11, 319.

Kraus, E.B., and J.S. Turner (1967). A one-dimensional model of the seasonal thermocline. II. The general theory and its consequences. *Tellus* 19, 98-106.

Rochford, D.J. (1951). Studies in Australian estuarine hydrology I: Introduction and comparative features. *Aust. J. mar. Freshwat. Res.* 2, 1-116.

Rochford, D.J. (1959). Classification of Australian estuarine systems. *Arch. Oceanogr. Limnol.* 11, 171-177.

Turner, J.S. (1973). Buoyancy effects in fluids. (Cambridge University Press: Cambridge).

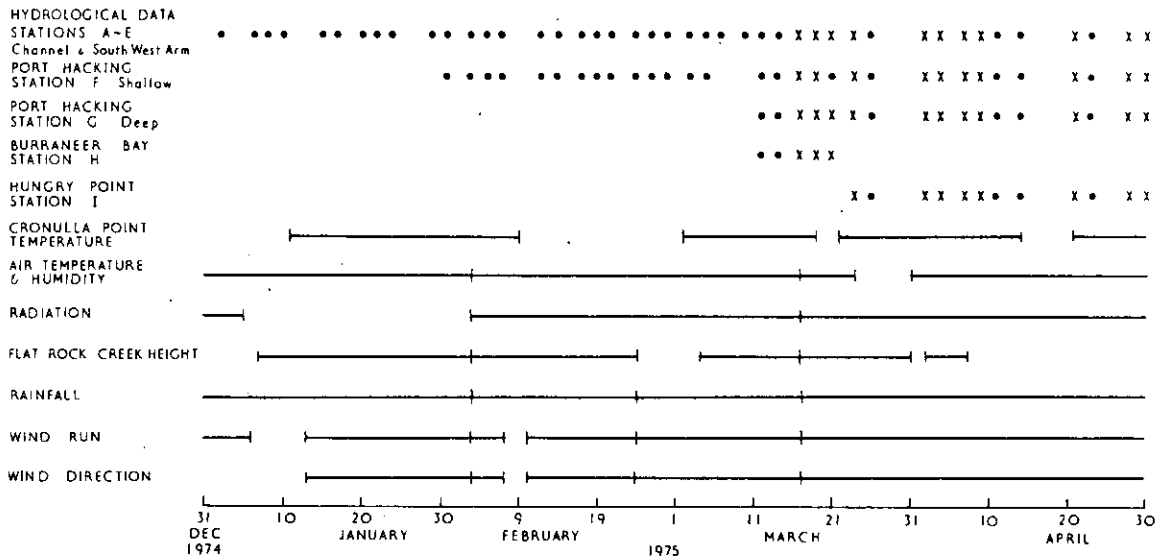

Fig. 11a. Data availability, Port Hacking study, 1.1.75 to 30.4.75. (x) indicates that salinity, temperature and dissolved oxygen data is available on the indicated day; (•) indicates that salinity and temperature only are available. The continuous temperature records at Hungry Point are available in chart form, but they have not been digitized. Data on height of the Hacking River at Upper Causeway is available throughout the study period, from the University of New South Wales. The full lines (⟝⟞) in Fig. 11a indicate times when continuous-record data is available.

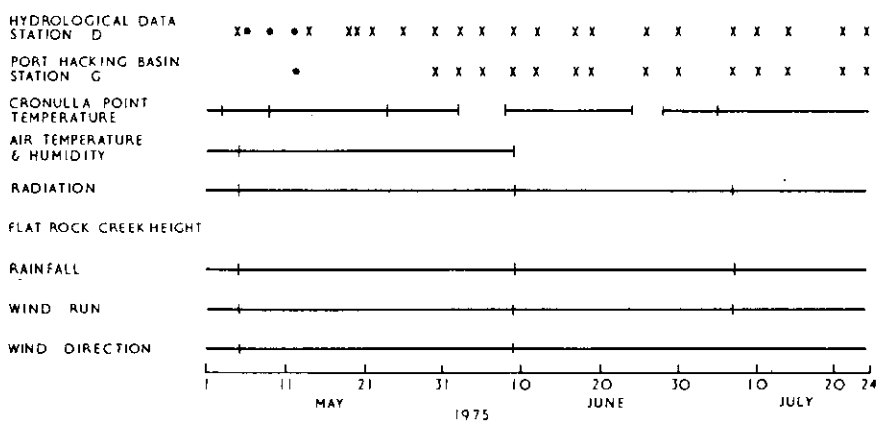

Fig. 11b. As for Fig. 11a, from 1.5.75 to 24.7.75.

APPENDIX

A1. HYDROLOGICAL DATA COLLECTION

Collection of data at a number of stations, 3 times a week, began on 1st September 1974 and is still continuing; however, we will describe here only the data collected between 10th January and 21st July 1975. Later data will be covered in a separate report, which will concentrate on describing the oxygen regime in Port Hacking. Within the period 10th January - 21st July, data were collected at stations A,B,C,...I, shown on Fig. 1. Not all the stations were occupied on all observation days, however; the dates on which data are available from each station are indicated in Fig. 11. Salinity and temperature were measured with a Hamon S/T meter, accurage to ± 0.1‰ and ± 0.1°C respectively, at depths of (0,1,2,4,6,8...) metres. All of these hydrological data have been stored on punched cards.

No attempt was made to collect the data at a particular state of the tide; it was generally collected between 7 a.m. and 10 a.m.

A2. METEOROLOGICAL DATA COLLECTION

It was not possible to install a meteorological station at South West Arm, so instead it was located at Cronulla. Rainfall was recorded using a Hellman-type recording raingauge. Wind run and direction were measured with a Mark II Sumner wind recorder; air temperature and humidity with a Casella thermohygrograph; and solar radiation with an Eppley pyranometer. Further details, including discussion of errors, will be found in a separate report, available on request. For present purposes, it suffices to note that instrumental errors can probably be neglected, compared to the errors induced by locating the station at Cronulla rather than at South West Arm. The data charts were digitized at two hourly intervals, from January 1975. There are some gaps in the records; data availability is indicated in Fig. 11.

A3. RIVER RUNOFF DATA

Daily outflow at Audley can be estimated by taking the discharge of the Port Hacking River, 9 km upstream from Audley at the Upper Causeway, and multiplying the result by an empirical factor (1.5) to allow for catchment area differences. It is thought that the resultant daily discharge figures should be accurate to about 20%, but this has not been adequately checked by direct measurements.

The data are made available by courtesy of Dr I. Cordery and Mr D. Doran, University of New South Wales Civil Engineering Department; the University of New South Wales records go back to 1961. However, at present the processing of the raw river height data (by the author) to obtain discharge figures is laborious and inaccurate, and so only the results for one period of particular interest is shown in Fig. 4a. A computer-based processing scheme is under development at the University of New South Wales.

Flat Rock Creek was also gauged (by the author), but this operation was largely unsuccessful. However, data were gathered during the storm of 10th - 13th March, 1975 and the few days preceding and following it. During this period, daily discharge of Flat Rock Creek varied between 0.15 and 0.3 times that of the Port Hacking River at Audley. This is roughly the ratio to be expected on the basis of the catchment area ratio.

A4. TIDE HEIGHT DATA

A Sumner water level recorder was installed in South West Arm, south of Gogerly's Point, May - June 1973. A tide height prediction program was developed from an analysis of two 29-day periods, using standard techniques. Spot checks have been made on a number of occasions since then, and the predictions have generally been accurate to ± 10 cm. Information on tide heights and delays in other parts of Port Hacking come from a Survey by the New South Wales Department of Public Works, 1969: Cat. No. 857, "Port Hacking — General Plan and Tidal Gradient".

A5. OTHER DATA

Apart from the "formal" data collection described above, a number of special observing trips were made, as opportunity arose. These trips, of 10 - 12 hour duration, generally yielded much more useful information per man-hour of effort than any of the other observational strategies used.

On several of these trips, the strategy was completely free-wheeling; features of particular interest — fronts, orientation of boats at anchor in still weather, orientation of seagrass blades, motion of debris, etc. — were noted, and investigated using an S/T meter and pellets of fluorescein. On other trips, specific features were investigated, particularly the tidal cycle of temperature and salinity in the main channel, in the two inner basins and in Bate Bay. In two other trips, S/T and current meter observations were made at several points around the entrance to South West Arm, over a tidal cycle.

In another expedition strips of fluorescein-soaked egg carton were put into the lay of a mooring line, and the streaks laid out at various depths observed by diving. "Informal" data collection of this kind is essential for the proper interpretation of the basic data series.